Electrospun Scaffolds Limit the Regenerative Potential of the Airway Epithelium

Cynthia M. Schwartz, MD; Jacob Stack; Cynthia L. Hill, BS; Scott W. Lallier, BS; Tendy Chiang, MD ⓘ;
Jed Johnson, PhD; Susan D. Reynolds, PhD ⓘ

Objective: Significant morbidity and mortality are associated with clinical use of synthetic tissue-engineered tracheal grafts (TETG). Our previous work focused on an electrospun polyethylene terephthalate and polyurethane (PET/PU) TETG that was tested in sheep using a long-segment tracheal defect model. We reported that graft stenosis and limited epithelialization contributed to graft failure. The present study determined if the epithelialization defect could be attributed to: 1) postsurgical depletion of native airway basal stem/progenitor cells; 2) an inability of the PET/PU-TETG to support epithelial migration; or 3) compromised basal stem/progenitor cell proliferation within the PET/PU environment.
Study Design: Experimental.
Methods: Basal stem/progenitor cell frequency in sheep that underwent TETG implantation was determined using the clone-forming cell frequency (CFCF) method. A novel migration model that mimics epithelial migration toward an acellular scaffold was developed and used to compare epithelial migration toward a control polyester scaffold and the PET/PU scaffold. Basal stem/progenitor cell proliferation within the PET/PU scaffold was evaluated using the CFCF assay, doubling-time analysis, and mitotic cell quantification.
Results: We report that TETG implantation did not decrease basal stem/progenitor cell frequency. In contrast, we find that epithelial migration toward the PET/PU scaffold was significantly less extensive than migration toward a polyester scaffold and that the PET/PU scaffold did not support basal stem/progenitor cell proliferation.
Conclusions: We conclude that epithelialization of a PET/PU scaffold is compromised by poor migration of native tissue-derived epithelial cells and by a lack of basal stem/progenitor cell proliferation within the scaffold.
Key Words: Airway epithelium, tissue-engineered tracheal graft, stem, progenitor, migration.
Level of Evidence: NA

INTRODUCTION

Long-segment tracheal defects are rare but life-threatening conditions. Such defects are caused by congenital or acquired etiologies, including complete tracheal rings, laryngotracheal agenesis, iatrogenic stenosis from prolonged endotracheal intubation, and secondary defects from malignancy and infection.[1] Tissue-engineered tracheal grafts (TETG) have the potential to cure these defects. However, TETG trials in human patients

identified multiple complications, including infection, inflammation, and stenosis.[1–3]

The conducting airway epithelium functions as a physical and chemical barrier that protects the lung from environmental agents.[4] Implantation of a TETG interrupts the epithelial barrier and a persistent epithelial gap fosters the aberrant wound-healing process that leads to poor outcomes. Improved TETG epithelialization has the potential to improve clinical outcomes. However, the mechanisms that impede the epithelialization process are not known.

The human and sheep conducting airway epithelium consists of several differentiated cell types, including columnar ciliated cells, goblet cells, and pyramidal basal cells.[5] Many studies indicate that the basal cell self-renews and serves as a multipotential progenitor for ciliated and goblet cells.[6–15] Thus, the basal cell is a stem/progenitor cell that maintains the healthy airway epithelium. Following an injury, the epithelium migrates toward the wound[16] and basal stem/progenitor cells generate the differentiated cells that restore epithelial function.

The present study focused on the electrospun polyethylene terephthalate and polyurethane (PET/PU) TETG that was previously evaluated in human patients[17] and sheep.[18,19] This TETG mimics the biomechanical properties of the human trachea.[20] However, in vivo studies demonstrated that PET/PU TETG, like other artificial scaffolds, did not epithelialize. Given the important contribution of basal stem/progenitor cells to epithelial

maintenance and repair, we determined if poor TETG epithelialization could be attributed to: 1) postsurgical depletion of native airway basal stem cells; 2) an inability of the PET/PU-TETG to support epithelial migration; or 3) compromised basal stem/progenitor cell proliferation in the PET/PU environment.

Our studies used the clone-forming cell frequency (CFCF) assay to determine basal stem/progenitor cell frequency in the postoperative airway and to determine if the PET/PU scaffold supported basal stem/progenitor cell clone formation. The CFCF assay is a variation of the limiting dilution method[21] and reports stem/progenitor cell frequency as the CFCF × 1,000. For example, a CFCF × 1,000 that equals 1,000 indicates that all test cells formed a clone. If the CFCF × 1,000 is 500, only half the test cells generated a clone. This assay has been used to quantify basal stem/progenitor cell frequency in vivo and in vitro.[8,22–24]

We also used air-liquid interface (ALI) cultures to model the host airway epithelium.[25–27] These cultures utilize a semi-porous polyester (PE) scaffold (Transwell membrane) to support basal stem/progenitor cell attachment, proliferation, and differentiation. At early time points (ie, differentiation day 2), ALI cultures exhibit a partially differentiated phenotype that is representative of the repairing epithelium.[28] At later time points (ie, differentiation day 21), ALI cultures acquire a well-differentiated phenotype that models the normal epithelium. Our work and that of others indicates that the PE scaffold supports epithelial migration and wound closure.[29–31] To evaluate epithelial migration toward the acellular PET/PU scaffold, we developed a method that adheres ALI cultures to a second scaffold. We used this model system to compare epithelial migration toward a PE control scaffold and a PET/PU test scaffold.

MATERIALS AND METHODS

Animal Subjects

The procedures employed in this study were reviewed and approved by the Nationwide Children's Hospital Institutional Animal Care and Use Committee.

Sheep Tracheal Cell Recovery

Cells were recovered from a 5 cm segment of sheep trachea (~5–6 cartilage rings) as previously reported.[27] Epithelial and fibroblast cell types were selected as previously reported.[23]

Surgical Implantation of a TETG in a Lamb Model

Surgical methods were previously described.[18] On postoperative days 6, 12, and 24, an optical forceps was used to biopsy the native tracheal epithelium ~2–3 cm above or below the anastomoses and tissue at the distal and proximal anastomoses. Cells were recovered as previously reported.[27]

Modified Conditional Reprogramming Cell Culture Method

The modified conditional reprogramming cell (mCRC) method is a variation of the Schlagel CRC method.[32] Importantly, the mCRC method makes use of nonproprietary irradiated feeder cells. This study used NIH3T3 (ATCC, Manassas, VA, CRL-1658) or sheep primary fibroblasts. The cell type used as an irradiated fibroblast feeder layer is indicated in "Results" section. Feeder cells were irradiated with 3,000 rad delivered by an X-irradiator (Precision XRay X-Rad 320 Irradiator). The mCRC methods also employ the ROCK inhibitor Y27632 (Stem Cell Technologies). To determine the effect of Y26632 on clone formation, test cell density was increased to 6.7×10^5 cells/cm^2 and Y27632 was replaced by vehicle dimethyl sulfoxide (DMSO).

Burst Size and CFCF Determination

The burst size and CFCF were quantified as previously reported.[23]

Cell Phenotype Determination

Cytospin preparations or transwell membranes were immunostained for Keratin 5 (1:1,000, Biolegend PRB-160P-905501), Keratin 14 (1:500, Invitrogen, MA5-11599), and/or β-Catenin (1:250, BD Transduction Laboratories, #610154). Nuclei were stained with 1 μg/mL 4′,6-diamidino-2-phenylindole (DAPI, Sigma, D9542-5mg) as previously reported.[23] The frequency of cells expressing Keratin 5 or Keratin 14 was reported as 100x (number immuno-positive cells/number DAPI positive cells).

Electrospun PET/PU Plate Fabrication

Cell culture plates were manufactured by Nanofiber Solutions (Hilliard, OH). Polymers were 20% polyethylene terephthalate (PET) and 80% polyurethane (PU). The PET/PU solution was electrospun onto a polystyrene (PS) sheet and the PS film was then cut to fit onto the bottom of 12-, 24-, or 96-well plates. Thus, the PET/PU scaffold was located on the culture surface. A 30 second radio frequency plasma treatment was applied to the plates and they were sterilized by ultraviolet irradiation.

Migration Studies

ALI cultures were generated using previously published methods.[28] Scratch wound studies were conducted as previously described[29] using partially differentiated (day 2) or well-differentiated (day 21) cultures. Each study evaluated migration in cultures derived from four donors with six technical replicates per donor. Studies evaluating migration toward the 4.67 cm^2 PE (Costar Transwell membrane, 3450) or PET/PU scaffolds utilized differentiation day 2 ALI cultures as the test epithelium. As detailed in "Results" section, the test epithelial culture was adhered to the test scaffold with 0.05 μL 2-octyl cyanoacrylate (Surgi-Lock, Meridian, Allegan, MI). The epithelium/scaffold constructs were incubated in differentiation medium until the indicated time point.

Lactate Dehydrogenase Release Assay

The lactate dehydrogenase (LDH) assay (Fisher #88953) was performed according to the manufacturer's directions.

Quantification of Migration

Constructs were imaged using an Aperio ScanScope FL (Leica Biosystems, Illinois, USA). ImageJ (National Institutes of Health, Bethesda, Maryland, USA) was used to trace the perimeter of the test epithelium and the migratory front. These data were used to compute the migratory area (A_o) and the area of the

test epithelium (A_i). A_i was subtracted from A_o to obtain the area of the migratory front. To calculate the migratory velocity (V_{mig}), the square root of the average migratory area at three time points was fit with a linear regression. The slope (m) from the linear regression fit was divided by 2.[30]

Doubling Time Analysis

Doubling time was calculated as: DT = $T(\ln2)/\ln(Xe/Xb)$, where DT is the doubling time, T is the incubation time in any unit, Xb is the cell number at the beginning of the incubation time, and Xe is the cell number at the end of the incubation time (https://www.atcc.org/~/media/PDFs/Culture%20Guides/AnimCellCulture_Guide.ashx).

Statistics

Statistical analyses were performed with GraphPad Prism version 7.00 for Windows (GraphPad Software, La Jolla California USA, www.graphpad.com). Descriptive statistics for continuous variables were presented as means and standard deviations. Normally distributed data sets were evaluated by Student's t test, and data sets that exhibited non-normal distributions were analyzed by the Mann–Whitney test. Data sets containing multiple variables were analyzed by analysis of variance and the post hoc Tukey test.

RESULTS

In Vitro Expansion of Sheep Tracheal Epithelial Cells

This study determined if the mCRC method could be used to expand sheep tracheal epithelial cells. P1 cultures
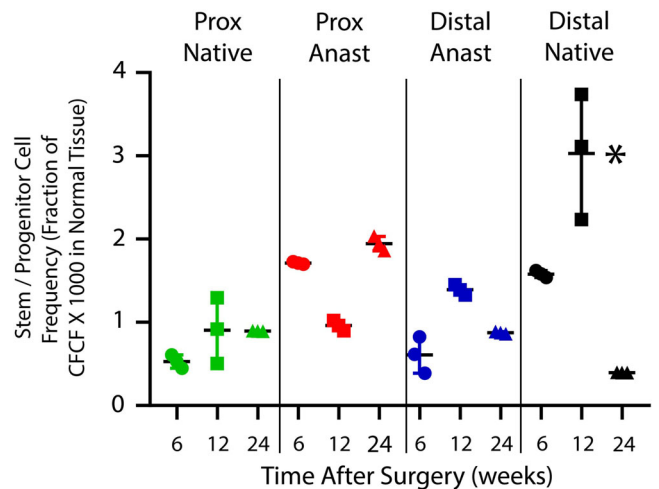

Fig. 2. Stem/progenitor cell frequency after tissue-engineered tracheal grafts (TETG) implantation. Basal stem/progenitor cell frequency was determined 6, 12, or 24 weeks after TETG implantation using the CFCF assay (A). Regions tested were the proximal (Prox) and distal (Dist) native tissue and the distal and proximal anastomoses (Anast). Data are presented as a fraction of the CFCF for normal tracheal tissue (mean ± standard deviation). Symbols represent the mean value for each of three donors. *P = .05 relative normal tracheal tissue. CFCF = clone-forming cell frequency.

yielded $2.79 \times 10^7 \pm 2 \times 10^4$ cells and the burst size was 1.7-fold. This cell amplification was within the range observed for P1 human airway epithelial cells.

The ROCK inhibitor Y27632 significantly increases the burst size and preserves human airway epithelial
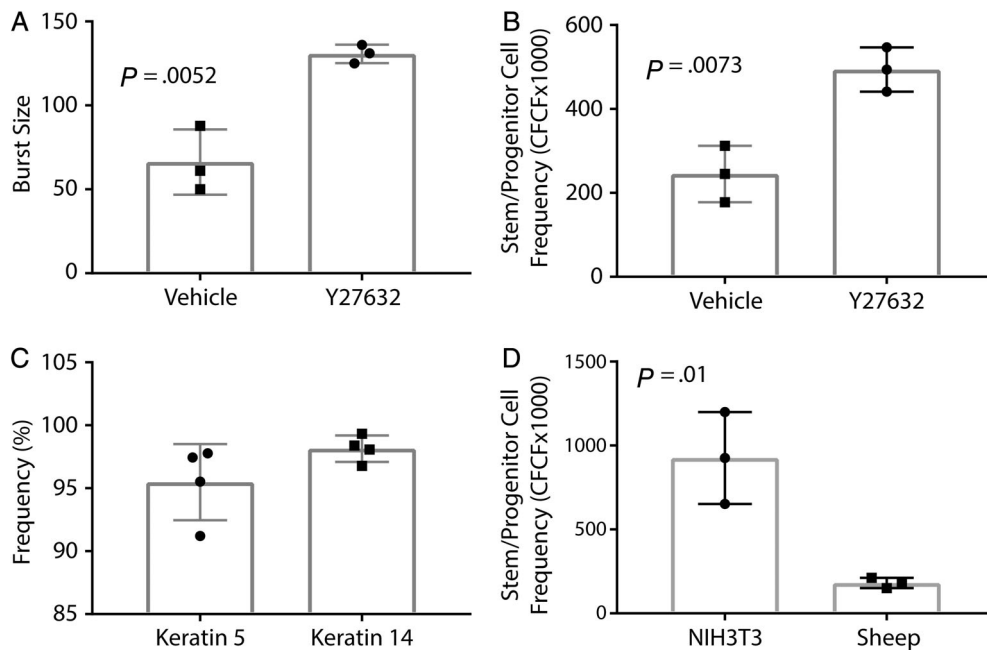

Fig. 1. In vitro expansion of sheep tracheal epithelial cells. P1 sheep tracheal basal stem/progenitor cells were cultured using the mCRC method. Cell growth was evaluated by determining the burst size (A) and the stem/progenitor cell frequency using the CFCF assay (B). Basal stem/progenitor cell phenotype was determined by immunostaining for basal cell markers, Keratins 5 and 14 (C). The impact of feeder layer cell type on CFCF was determined by culturing basal stem/progenitor cells on NIH3T3 or sheep fibroblast feeder layers (D). Data are presented as the mean ± standard deviation. Symbols represent the mean value for each of 3–4 donors. CFCF = clone-forming cell frequency; mCRC = modified conditional reprogramming cell.

stem/progenitor cell number.[23,24] To determine if Y27621 altered sheep cell burst size, P1 sheep tracheal cells were cultured on irradiated NIH3T3 feeder cells in FMED containing vehicle (DMSO) or 10 µM Y27632. At P2, epithelial cells were recovered and counted. Addition of Y27632 significantly increased the burst size by a factor of 2 (P = .0052, Fig. 1A).

To determine if Y27621 altered stem/progenitor cell frequency, P1 sheep tracheal cells were quantified according to the CFCF method. Cells were cultured on irradiated NIH3T3 feeder cells in FMED containing DMSO or 10 µM Y27632. On culture day 9, the cultures were fixed, stained, and scored. Addition of Y27632 significantly increased the progenitor cell frequency by a factor of 2 (P = .0073, Fig. 1B).

Human airway epithelial stem/progenitor cells express Keratins 5 and 14 in vitro. To determine if the mCRC culture method selected for sheep tracheal epithelial stem/progenitor cells, P2 sheep cells were used to
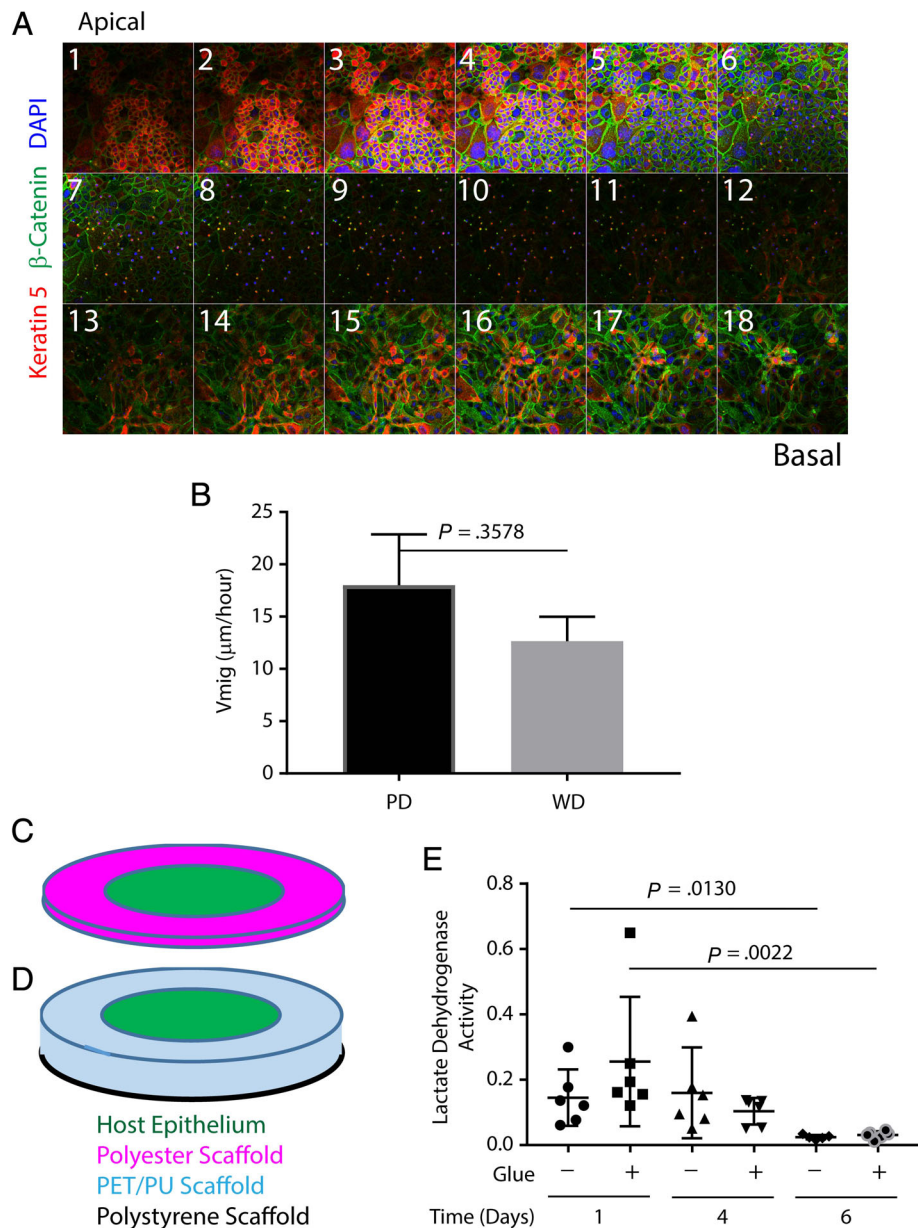

Fig. 3. Epithelial migration model development. Epithelial migration on a polyester (PE) scaffold containing 8.0 micron pores was evaluated using confocal microscopy (A). A montage of 18 images spanning the apical (upper left) and basal (lower right) aspects of the membrane is presented. Red: Keratin 5, green: β-catenin, and blue: DAPI. Basal stem/progenitor cells were cultured on PE scaffold containing 0.4 micron pores. A scratch wound was generated in the partially differentiated (PD) or well-differentiated (WD) epithelium and migratory velocity (V_{mig}) was quantified (B). Cartoons representing the constructs used to model epithelial migration toward an acellular PE/0.4 micron scaffold (C) or a PET/PU scaffold (D). Green disk, host epithelium; pink disk, PE scaffold; blue disk, PET/PU scaffold; black disk, polystyrene scaffold. The impact of octyl-cyanoacrylate glue on epithelial cell viability was determined using the lactate dehydrogenase activity assay (E). Data are presented as the mean ± standard deviation. Symbols represent the value for each of six samples. DAPI = 4′,6-diamidino-2-phenylindole; PET/PU = polyethylene terephthalate and polyurethane.

Schwartz et al.: Synthetic Graft Epithelialization

generate cytospins and immunostained for Keratins 5 and 14. These cells were 95% ± 3% Keratin 5 positive and 98% ± 1% Keratin 14 positive (Fig. 1C). These data indicate that the mCRC cultures were highly enriched for basal cells and that the mCRC method can be used to expand sheep tracheal basal stem/progenitor cells.

A previous study demonstrated that human airway epithelial stem/progenitor cells were maintained by multiple fibroblast feeder cell types and that progenitor cell frequency was not influenced by feeder cell species, developmental stage, or disease.[23] To determine if sheep primary fibroblast feeder layers affected basal stem/progenitor cell
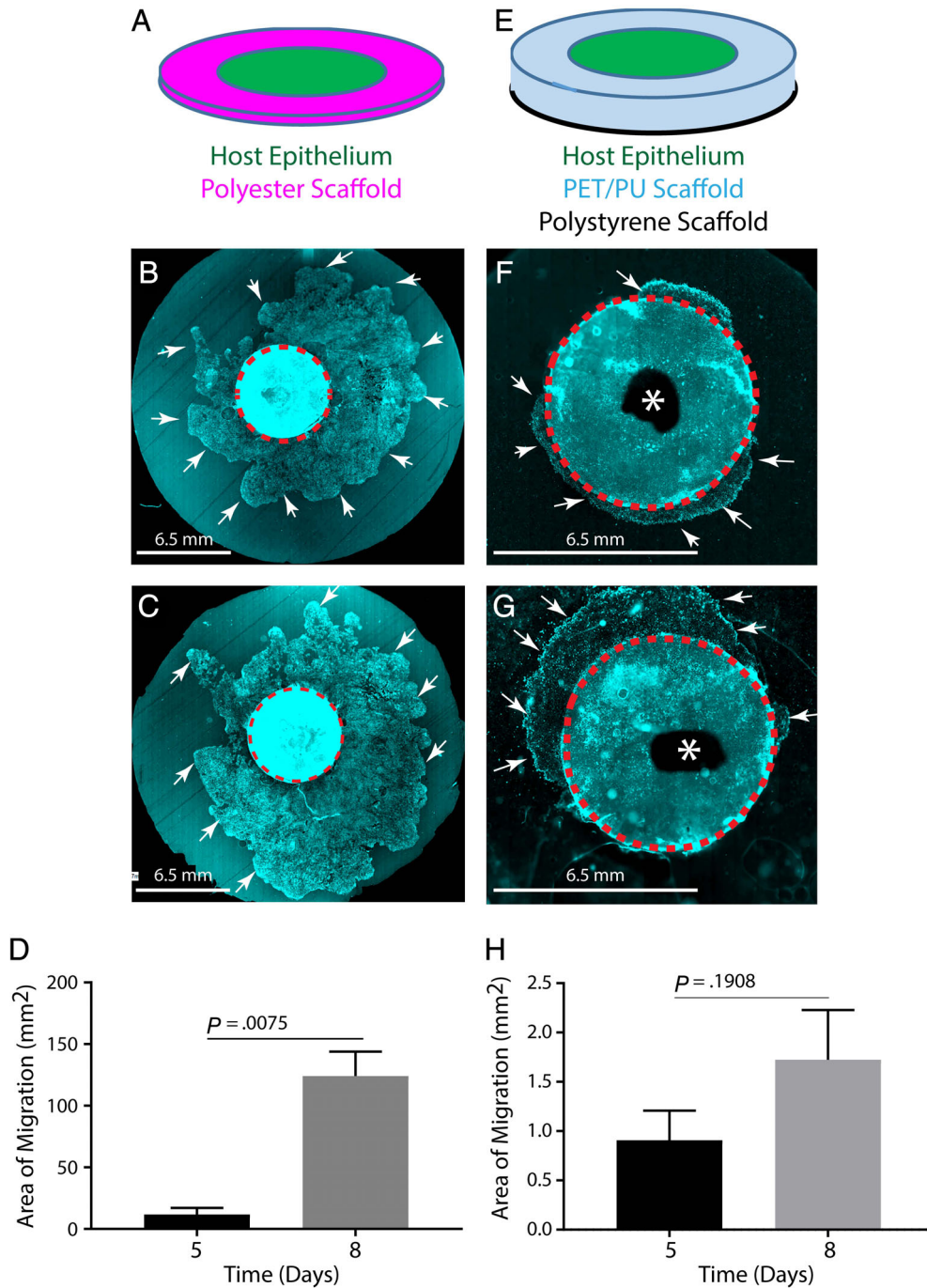

Fig. 4. Epithelial migration toward acellular scaffolds. Epithelial migration across a polyester scaffold containing 0.4 micron pores (A) was evaluated using standard microscopy on days 5 (B) and 8 (C). Dashed red line: perimeter of the host epithelium. Arrows: Edge of the migrating epithelium. The area of migration was determined as a function of time (D). Data are presented as the mean ± standard deviation (n = 3 donors). Epithelial cell migration toward a PET/PU scaffold (E) was evaluated using standard microscopy on days 5 (F) and 8 (G). Dashed red line: perimeter of the host epithelium. Arrows: Edge of the migrating epithelium. Asterisk: Pen mark used to indicate the center of the host epithelium. The area of migration was determined on days 5 and 8 (H). Data are presented as the mean ± standard deviation (n = 6 samples). PET/PU = polyethylene terephthalate and polyurethane.

maintenance, basal stem/progenitor cell frequency was compared in mCRC cultures containing NIH3T3 or sheep fibroblast feeder layers. Stem/progenitor cell frequency was significantly greater in cultures containing NIH3T3 feeder layers (P = .01, Fig. 1D). These data indicate that NIH3T3 feeder layers are optimal for propagation of sheep basal stem/progenitor cells.

Stem/Progenitor Cell Frequency after PET/PU TETG Implantation

To determine if surgical placement of a PET/PU TETG altered basal stem/progenitor cell frequency, the native epithelium and anastomotic sites were sampled on postoperative weeks 6, 12, and 24. Basal stem/progenitor cell frequency in the proximal native and anastomotic tissue samples was within the normal range at each time point (Fig. 2). Although basal stem/progenitor cell frequency was significantly increased in the distal native airway at the 12 week time point (Fig. 2), stem/progenitor cell frequency was within the normal range at the other two time points. These data indicate that basal stem/progenitor cell frequency did not decrease in response to surgical implantation of a PET/PU TETG.

Epithelial Migration Model

A potential explanation for suboptimal TETG epithelialization in vivo was that the native epithelium did not migrate toward the PET/PU scaffold. To address this question, we developed a system that modeled epithelial migration toward a test scaffold. First, we determined if basal stem/progenitor cells migrated through a PE scaffold. A single cell suspension of basal stem/progenitor cells was seeded onto the apical surface of PE transwell membranes that contained 8.0 micron pores. Confocal microscopy on culture day 7 demonstrated formation of a confluent epithelium on both the apical and basal surfaces of the PE scaffold (Fig. 3A). These data indicate that PE is an appropriate substrate for epithelial migration and that epithelial cells migrated through 8.0 micron pores.

Next, we determined if epithelial migration was dependent on the extent of differentiation. ALI cultures were established on PE transwell membranes (0.4 micron pores) according to standard methods, differentiated to the partial and well-differentiated stages, and wounded with a 0.8 mm stylus. This study demonstrated that the rate of migration did not vary between partially differentiated and well-differentiated cultures (Fig. 3B) and allowed us to model epithelial migration with partially differentiated ALI cultures.

Finally, we developed a system that modeled migration of the native epithelium toward a TETG (Fig. 3C, 3D). Partially differentiated epithelia were generated on 0.33 cm^2 PE membranes, excised from the culture vessel, and placed on the surface of the test scaffold or adhered to the scaffold with 2 octyl-cyanoacrylate glue. To determine if the excision/gluing process damaged the test epithelium, cellular damage was quantified using the LDH assay. LDH activity was increased on culture days 1 and 2 relative to day 6 (Fig. 3E). However, LDH activity did not vary between the no glue and glue conditions.

Epithelial Migration Toward PE and PET/PU Test Scaffolds

To determine if the test epithelium migrated toward a PE/0.4 micron pore (PE/0.4) scaffold (Fig. 4A), we measured the area of migration on days 5 (Fig. 4B) and 8 (Fig. 4C). The area of migration increased significantly over time (P = .0075, Fig. 4D). Next, we investigated epithelial migration toward the PET/PU scaffold (Fig. 4E–G). On culture day 5, epithelial migration toward the PET/PU
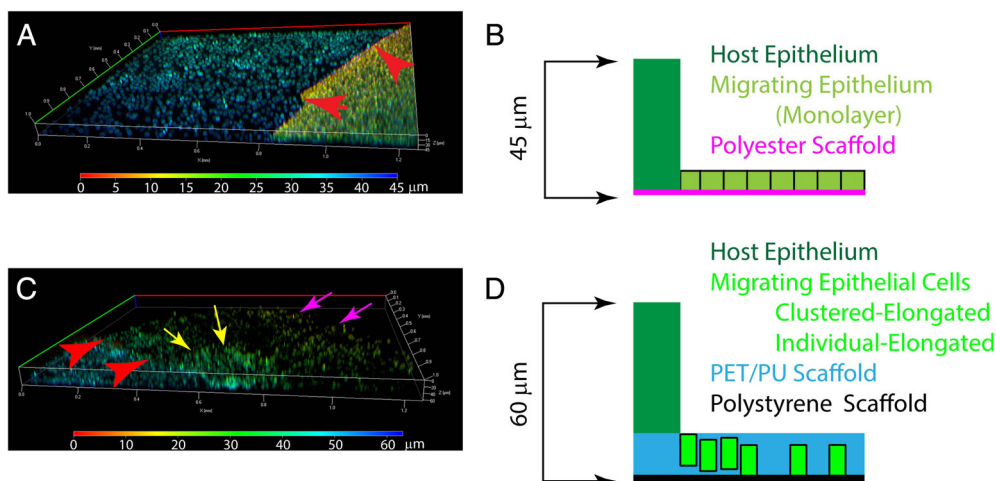

Fig. 5. Morphology of epithelia that are migrating toward acellular scaffolds: Confocal imaging and three-dimensional reconstruction were used to evaluate the spatial relationship between the host and migratory epithelium. Migration toward a polyester (PE) scaffold containing 0.4 micron pores (A). Colors indicate a cell's position within the Z-axis. Red arrows: edge of the host epithelium. A cartoon representing the relationships between the host epithelium (dark green), migrating epithelium (light green), and the PE scaffold (pink) (B). Migration toward a PET/PU scaffold (C). Colors indicate cell position within the Z-plane. Arrows: red, edge of the host epithelium; yellow, clusters of migrating cells; pink, single migrating cells. A cartoon representing the relationships between the host epithelium (dark green), migrating epithelial cells (light green), the PET/PU scaffold (blue), and the polystyrene scaffold (black) (D). PET/PU = polyethylene terephthalate and polyurethane.

scaffold was detected in constructs from four of five donors. However, the area of migration did not increase over time (Fig. 4H). Overall, the average area of migration was ~10-fold greater for PE/0.4 scaffolds on days 5 and 8 ($P < .001$, compare Fig. 4D, 4H). These data indicate that epithelial migration toward the PET/PU scaffold was significantly less than migration toward the PE/0.4 scaffold.

A confocal microscopy study (Fig. 5A, 5B) demonstrated that migratory epithelial cells formed a monolayer on the apical surface of the PE/0.4 scaffold and that these cells were in contact with the host epithelium. Epithelial cells were not detected on the basal surface of the test PE/0.4 scaffold. A parallel analysis of cells migrating toward the PET/PU scaffold (Fig. 5C, 5D) demonstrated that migratory epithelial cells were clustered within the

scaffold or attached to the polystyrene surface of the well. Cells at each of these locations exhibited an elongated morphology. Epithelial cells were not observed on the surface of the PET/PU scaffold. Collectively, these data demonstrate that the PE/0.4 scaffold supported formation of a nascent epithelium. In contrast, epithelial migration toward the PET/PU scaffold was transient and did not result in formation of an epithelial structure.

Maintenance and Growth of Basal Stem/Progenitor Cells by the PET/PU Scaffold

Our final goal was to determine if the PET/PU scaffold supported basal stem/progenitor proliferation. First, we used confocal imaging to evaluate the structural
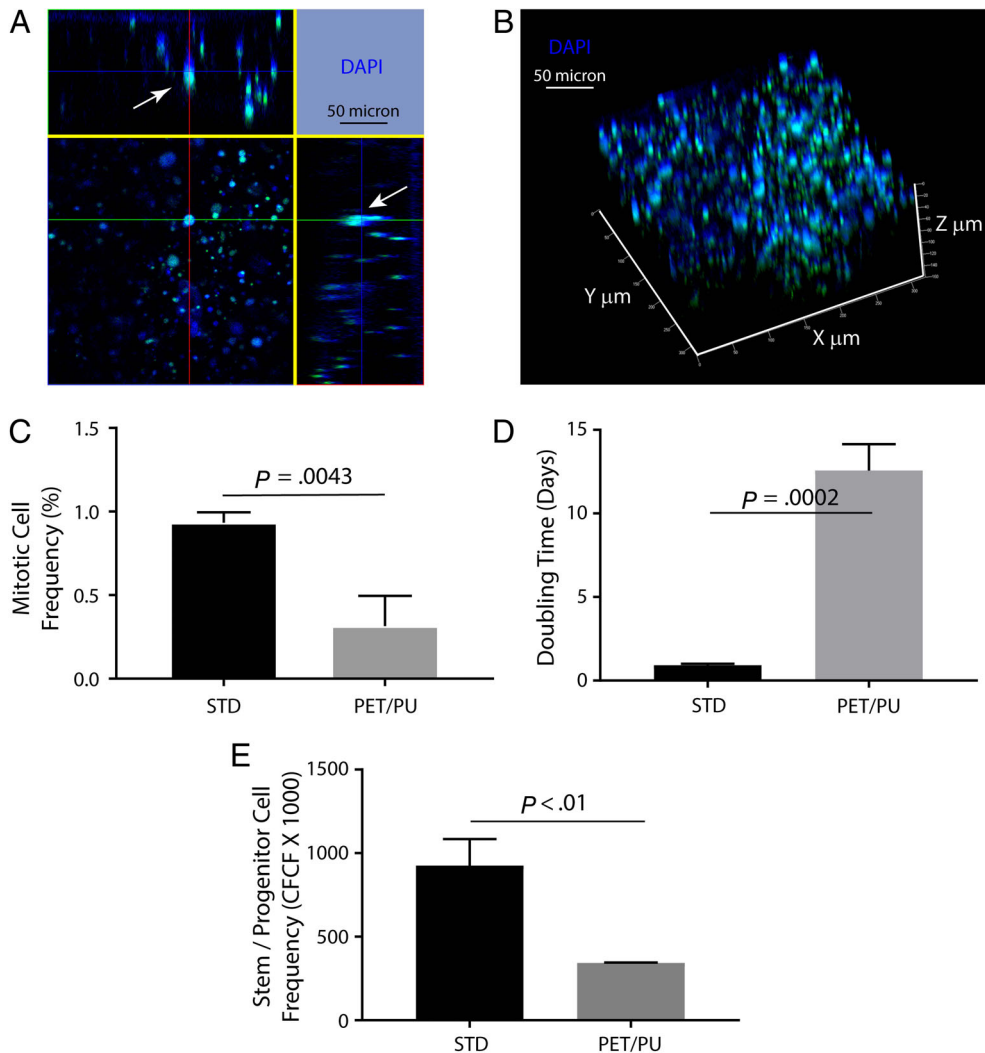

Fig. 6. Maintenance and growth of epithelial stem/progenitor cells that are cultured on the PET/PU scaffold. P1 sheep stem/progenitor cells were seeded into cell culture plates containing a tissue-engineered tracheal grafts scaffold. Confocal imaging was used to evaluate epithelial structure at 1 week (A, orthogonal presentation) and at 2 weeks (B, three-dimensional presentation). Blue: DAPI; Green: cellular autofluorescence. Mitotic cell frequency was determined for cells that were cultured under standard (STD) conditions or on PET/PU scaffolds (C). Doubling time was determined for cells cultured under STD or PET/PU conditions (D). Basal stem/progenitor cell frequency was assayed using the clone-forming cell frequency (CFCF) assay. Data are presented as the mean ± standard deviation (n = 3 donors). CFCF = clone-forming cell frequency; DAPI = 4',6-diamidino-2-phenylindole; PET/PU = polyethylene terephthalate and polyurethane.

characteristics of basal stem/progenitor cells that were seeded onto the PET/PU scaffold in vivo. At early time points (1 week), the cultures contained individual cells that were elongated (~5 μm wide and ~20 μm tall, Fig. 6A). The nucleus was positioned in the apical portion of the cell. At later time points (2 weeks), the cells grew in discrete columns and retained the apical nuclear position (Fig. 6B). Importantly, epithelial sheets were not observed at either time point. This morphology was in stark contrast with the morphology of cells grown on polyester scaffolds.

To determine if basal stem/progenitor cells proliferated within in the PET/PU environment, we compared the mitotic cell frequency of basal stem/progenitor cells that were cultured under standard conditions or in the PET/PU scaffold. We found that mitotic cell frequency was significantly greater in standard cell cultures (Fig. 6C). Next, we compared the doubling time and found that doubling time was significantly greater in PET/PU cultures (Fig. 6D). Finally, we used the CFCF assay to compare basal stem/progenitor cell frequency in standard or PET/PU cultures. This study demonstrated that basal stem/progenitor cell frequency was significantly greater in standard cultures relative to PET/PU cultures (Fig. 6E). Collectively, these data indicate that the PET/PU scaffold was not an optimal environment for basal stem/progenitor cell proliferation.

DISCUSSION

Clinically Relevant Models for Preclinical Testing

Development of next generation TETG may be facilitated through use of in vitro model systems that mimic the native tissue, the TETG scaffold, and interactions between the native tissue and the scaffold. The present study developed two methods that will enable this type of preclinical testing. First, we demonstrate that the mCRC culture method allows selection and expansion of basal stem/progenitor cells from the sheep trachea (Fig. 1). Use of sheep stem/progenitor cells will enable translation of in vitro studies to repair of long segment defects in the sheep model. Second, we developed a novel migration model (Figs. 3 and 4) that mimics the movement of an intact epithelium across an anastomosis. Since the epithelium is moving toward an acellular scaffold, this model represents the clinical situation more faithfully than the scratch wound assay. The adaptability of this model to various scaffold types and identification of a scaffold (PE/0.4) that supports robust epithelial migration will facilitate comparative analysis of new TETG prototypes.

Reparative Potential of the Postoperative Airway Epithelium

We demonstrate that TETG implantation had little or no impact on the frequency of basal stem/progenitor cells (Fig. 2). These data indicate that native airway basal stem/progenitor cells should be able to epithelialize the TETG. However, our in vitro studies indicate that the PET/PU scaffold does not support epithelial migration (Fig. 4). Since migration was robust on the control PE scaffold, these studies indicate that the PET/PU scaffold limits the migratory capacity of the epithelium. Our in vitro studies also indicate that basal stem/progenitor cell proliferation was attenuated by the PET/PU scaffold (Fig. 6). Decreased proliferation could contribute to the migration defect and limit cellularization of the PET/PU scaffold in vivo. Finally, we observed that the PET/PU scaffold altered basal stem/progenitor cell morphology (Figs. 4 and 5). These changes, particularly the lack of cell-cell contacts that define epithelial sheet formation, are likely to impact both migration and proliferation. Collectively, these data indicate that TETG epithelialization in vivo is limited by the PET/PU scaffold rather than the regenerative potential of the native airway epithelium.

CONCLUSION

We conclude that epithelialization of a PET/PU scaffold is compromised by poor migration of native tissue-derived epithelial cells and by a lack of basal stem/progenitor cell proliferation within the scaffold.

BIBLIOGRAPHY

1. Chiang T, Pepper V, Best C, Onwuka E, Breuer CK. Clinical translation of tissue engineered trachea grafts. *Ann Otol Rhinol Laryngol* 2016;125: 873–885.
2. Law JX, Liau LL, Aminuddin BS, Ruszymah BH. Tissue-engineered trachea: a review. *Int J Pediatr Otorhinolaryngol* 2016;91:55–63.
3. Udelsman B, Mathisen DJ, Ott HC. A reassessment of tracheal substitutes—a systematic review. *Ann Cardiothorac Surg* 2018;7: 175–182.
4. Hamilton LM, Davies DE, Wilson SJ, Kimber I, Dearman RJ, Holgate ST. The bronchial epithelium in asthma—much more than a passive barrier. *Monaldi Arch Chest Dis* 2001;56:48–54.
5. Rock JR, Randell SH, Hogan BL. Airway basal stem cells: a perspective on their roles in epithelial homeostasis and remodeling. *Dis Model Mech* 2010;3:545–556.
6. Ghosh M, Ahmad S, White CW, Reynolds SD. Transplantation of airway epithelial stem/progenitor cells: a future for cell-based therapy. *Am J Respir Cell Mol Biol* 2017;56:1–10.
7. Ghosh M, Brechbuhl HM, Smith RW, et al. Context-dependent differentiation of multipotential keratin 14-expressing tracheal basal cells. *Am J Respir Cell Mol Biol* 2011;45:403–410.
8. Ghosh M, Helm KM, Smith RW, et al. A single cell functions as a tissue-specific stem cell and the in vitro niche-forming cell. *Am J Respir Cell Mol Biol* 2011;45:459–469.
9. Hong KU, Reynolds SD, Watkins S, Fuchs E, Stripp BR. Basal cells are a multipotent progenitor capable of renewing the bronchial epithelium. *Am J Pathol* 2004;164:577–588.
10. Hong KU, Reynolds SD, Watkins S, Fuchs E, Stripp BR. In vivo differentiation potential of tracheal basal cells: evidence for multipotent and unipotent subpopulations. *Am J Physiol Lung Cell Mol Physiol* 2003;287: L643–L649.

11. Rock JR, Onaitis MW, Rawlins EL, et al. Basal cells as stem cells of the mouse trachea and human airway epithelium. *Proc Natl Acad Sci U S A* 2009;106:12771–12775.
12. Hegab AE, Ha VL, Darmawan DO, et al. Isolation and in vitro characterization of basal and submucosal gland duct stem/progenitor cells from human proximal airways. *Stem Cells Transl Med* 2012;1:719–724.
13. Hegab AE, Ha VL, Gilbert JL, et al. Novel stem/progenitor cell population from murine tracheal submucosal gland ducts with multipotent regenerative potential. *Stem Cells* 2011;29:1283–1293.
14. Lynch TJ, Anderson PJ, Rotti PG, et al. Submucosal gland myoepithelial cells are reserve stem cells that can regenerate mouse tracheal epithelium. *Cell Stem Cell* 2018;22:653–667.
15. Borthwick DW, Shahbazian M, Krantz QT, Dorin JR, Randell SH. Evidence for stem-cell niches in the tracheal epithelium. *Am J Respir Cell Mol Biol* 2001;24:662–670.
16. Puchelle E. Airway epithelium wound repair and regeneration after injury. *Acta Otorhinolaryngol Belg* 2000;54:263–270.
17. Gilevich IV, Polyakov IS, Porkhanov VA, Chekhonin VP. Morphological analysis of biocompatibility of autologous bone marrow mononuclear cells with synthetic polyethylene terephthalate scaffold. *Bull Exp Biol Med* 2017;163:400–404.
18. Pepper VK, Onwuka EA, Best CA, et al. Endoscopic management of tissue-engineered tracheal graft stenosis in an ovine model. *Laryngoscope* 2017; 127:2219–2224.
19. Clark ES, Best C, Onwuka E, et al. Effect of cell seeding on neotissue formation in a tissue engineered trachea. *J Pediatr Surg* 2015;51:49–55.
20. Best CA, Pepper VK, Ohst D, et al. Designing a tissue-engineered tracheal scaffold for preclinical evaluation. *Int J Pediatr Otorhinolaryngol* 2018; 104:155–160.
21. Taswell C. Limiting dilution assays for the determination of immunocompetent cell frequencies. I. Data analysis. *J Immunol* 1981;126:1614–1619.
22. Ghosh M, Smith RW, Runkle CM, Hicks DA, Helm KM, Reynolds SD. Regulation of trachebronchial tissue-specific stem cell pool size. *Stem Cells* 2013;31:2767–2778.
23. Reynolds SD, Rios C, Wesolowska-Andersen A, et al. Airway progenitor clone formation is enhanced by Y-27632-dependent changes in the transcriptome. *Am J Respir Cell Mol Biol* 2016;55:323–336.
24. Hayes D Jr, Kopp BT, Hill CL, et al. Cell therapy for cystic fibrosis lung disease: regenerative basal cell amplification. *Stem Cells Transl Med* 2018;8:225–235.
25. Wu R, Yankaskas J, Cheng E, Knowles MR, Boucher R. Growth and differentiation of human nasal epithelial cells in culture. Serum-free, hormone-supplemented medium and proteoglycan synthesis. *Am Rev Respir Dis* 1985;132:311–320.
26. Liu JY, Nettesheim P, Randell SH. Growth and differentiation of tracheal epithelial progenitor cells. *Am J Physiol* 1994;266:L296–L307.
27. You Y, Richer EJ, Huang T, Brody SL. Growth and differentiation of mouse tracheal epithelial cells: selection of a proliferative population. *Am J Physiol Lung Cell Mol Physiol* 2002;283:L1315–L1321.
28. Malleske DT, Hayes D Jr, Lallier SW, Hill CL, Reynolds SD. Regulation of human airway epithelial tissue stem cell differentiation by beta-catenin, P300, and CBP. *Stem Cells* 2018;36:1905–1916.
29. Schwartz CM, Dorn BA, Habtemariam S, Hill CL, Chiang T, Reynolds SD. The wound healing capacity of undifferentiated and differentiated airway epithelial cells in vitro. *Int J Pediatr Otorhinolaryngol* 2018;112:163–168.
30. Liang CC, Park AY, Guan JL. In vitro scratch assay: a convenient and inexpensive method for analysis of cell migration in vitro. *Nat Protoc* 2007;2: 329–333.
31. Jonkman JE, Cathcart JA, Xu F, et al. An introduction to the wound healing assay using live-cell microscopy. *Cell Adh Migr* 2014;8:440–451.
32. Suprynowicz FA, Upadhyay G, Krawczyk E, et al. Conditionally reprogrammed cells represent a stem-like state of adult epithelial cells. *Proc Natl Acad Sci U S A* 2012;109:20035–20040.